Proceedings 10th NUMGE 2023
10th European Conference on Numerical Methods in Geotechnical Engineering
Zdravkovic L, Kontoe S, Taborda DMG, Tsiampousi A (eds)

https://doi.org/10.53243/NUMGE2023-220

Effect of the failure mode on the macro-response of pile groups

D.N. Gorini[1], L. Callisto[1]

[1] *Department of Structural and Geotechnical Engineering, Sapienza University of Rome, Rome, Italy*

ABSTRACT: This paper contributes to the generalisation of existing models that describe the multiaxial response of pile groups. Most of these models, including a specific model proposed by the Authors, assume that the foundation piles are rigidly connected to the raft. In this study, the multiaxial conditions of deep foundations are analysed by assuming a frictional disconnection at the pile-raft level, aimed at limiting the shear forces transferred to the superstructure under seismic loading. This objective is accomplished through numerical-aided limit analysis and using advanced finite-element analysis. The modifications on the failure loads obtained for the dissipative configuration are incorporated into a hyperplastic macroelement of the piled foundation system to provide a calculation tool capable to account for a disconnection at the piles-raft interface. The macroelement is implemented in OpenSees and the effectiveness of the frictional disconnection is tested on a case study of a multi-span girder bridge in which both the piers foundations and the abutments are provided with this base isolation device.

Keywords: deep foundations; multi-mode failure; macroelement; seismic isolation

1 INTRODUCTION TO FRICTIONALLY DISCONNECTED PILED FOUNDATIONS

Piles are widely used as a means for increasing the bearing capacity or reducing settlements of a foundation subjected to the gravity loads. In the design of piled foundations against earthquake loading, it may be convenient to reduce the horizontal capacity of the foundation in order to control the shear forces transferred to the superstructure during strong motion. An easily implemented solution consists in disconnecting the piles from the raft through the interposition of a dissipative layer, creating a frictional isolating device at the pile-raft contact.

Implementation of this strategy to real cases include the foundations of the Rion-Antirion cable-stayed bridge in Greece (Pecker, 2003) and of the Izmit Bay suspension bridge in Turkey (Zhang et al., 2013). For the latter case, Callisto and Gorini (2020) carried out coupled numerical analyses showing that the seismic performance of the friction foundations is strongly influenced by the presence of the pile inclusions in the soil and by the vertical component of ground motion.

Recently, some experimental investigations were carried out to study the seismic performance of disconnected piles. Ko et al. (2018) evidenced lower seismic-induced bending moment developing in disconnected piles compared to conventional layouts. Kim et al. (2019) pointed out the influence of the enhanced rocking response of frictionally disconnected piled foundations on the dynamic forces developing in the superstructure.

The seismic effectiveness of a dissipative pile-raft interface is profoundly affected by the multiaxial dynamic response of the superstructure and by the multi-directionality of the ground motion altering the available resistance at the soil-raft contact. In this regard, Gorini and Callisto (2019) proposed a design procedure for calibrating the frictional properties of the soil-raft interface and the mass of the raft accounting for the above factors.

This paper provides a view of the failure modes of frictionally disconnected piled foundations under multiaxial loading conditions. On this basis, a macroelement for disconnected piled foundations is developed, and the predicted ultimate loads are compared with the results of advanced numerical analyses. The effectiveness of the design solution is finally tested on the case study of a girder bridge, whose main characters are recounted in the following.

2 THE CASE STUDY

The soil-bridge layout is schematically shown in Figure 1 (Gorini and Callisto, 2022a). The deck rests on five supports, endowed with piled foundations. The layered subsoil has a shear wave velocity increasing with depth from 200 m/s at the foundation level of abutment A1 to 1000 m/s at the bedrock encountered at a depth of 95 m. The angle of shearing resistance of the soil layers ranges between 24° and 26° and the cohesion is equal to 10 kPa.

In the longitudinal direction the deck is only connected to piers P2 and P3, and to abutment A2 using viscous dampers, while it is rigidly connected with all the supports in the transverse direction.

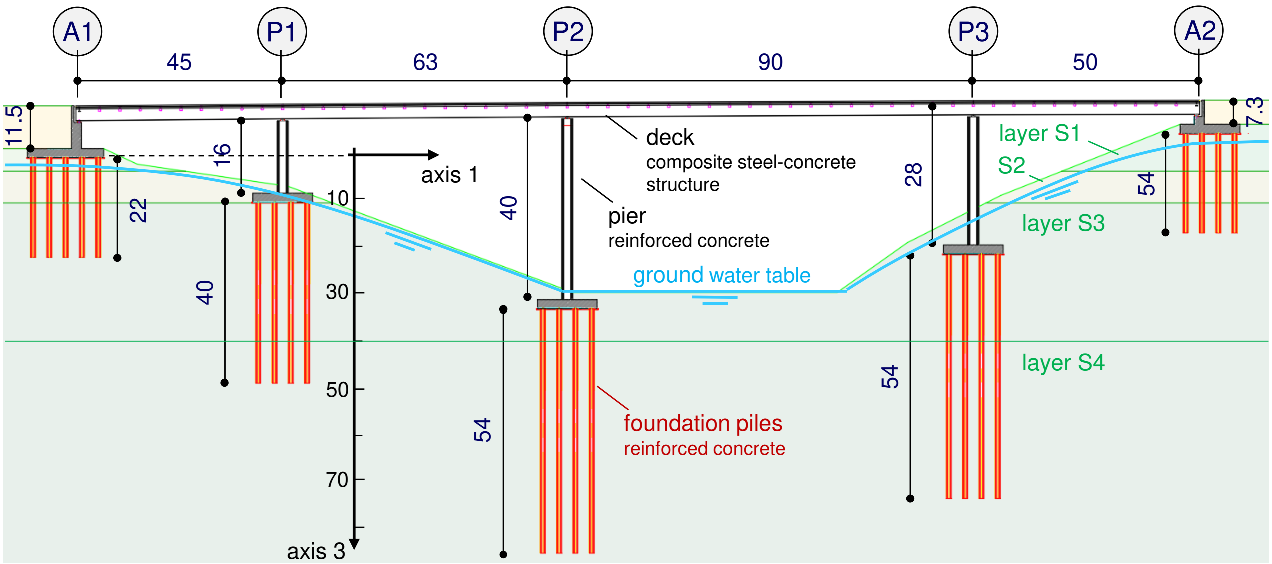

Figure 1. Longitudinal section of the reference soil-bridge system (lengths in meters).

For this case study, the original layout was modified introducing frictionally disconnected foundations at the piers and the abutments, assuming a friction angle of the dissipative layer $\varphi_{diss} = \varphi_s = 25°$. This was chosen using the design procedure outlined by Gorini and Callisto (2019) and according with the indications provided in Gorini et al. (2019) for the case of friction dissipative abutments.

3 FAILURE MODES OF DISSIPATIVE PILED FOUNDATIONS

3.1 Numerical procedure

The foundation of pier P2, shown in Figure 2, is used here as a reference for illustrating the modifications in the ultimate conditions of the foundation due to the interposition of the dissipative layer between piles and raft. The multiaxial loads transferred by the superstructure causing failure of the foundation were computed by referring to a recently developed numerical procedure, named DeepFUL, under the assumption of null vertical stresses transferred by the raft to the soil (Gorini and Callisto, 2022b). In brief, for a given loading path a pushover analysis is carried out in which, at each load step, the axial forces in the piles are updated accounting for the progressive attainment of the pile axial capacity. The yield bending moments of the piles cross-sections are a function of the computed axial forces, and the horizontal limit load is finally determined on the basis of an assumed failure mode for the piles. The procedure ends when a global plastic mechanism is detected, that may be due either to all piles reaching their vertical capacity or to a global horizontal failure (namely, vertical or horizontal load mechanism, respectively).

Some modifications were introduced in DeepFUL to consider the effects of the pile disconnection on the global failure modes. For the case study at hand, the horizontal failure of the connected piles is the usual fixed-head, long-pile mechanism implying two plastic hinges along the shaft (note that the diameter-to-length ratio of the piles is smaller than 2%). Conversely, for the frictionally disconnected foundations the horizontal failure mechanism is that of a free-head long-pile, with only one plastic hinge. The corresponding horizontal limit load of the single pile, $Q_1^{(\mathrm{lim},1)}$, can be computed using standard solutions.

In the dissipative layout, a horizontal load mechanism is produced by the lowest between the limit horizontal load of all piles, $Q_1^{(\mathrm{lim,G})}$, and the shearing resistance at the soil-raft contact, $Q_1^{(\mathrm{lim,S})}$. In turn, these limit loads are computed as $Q_1^{(\mathrm{lim,G})}=N\times\eta_H\times Q_1^{(\mathrm{lim},1)}$, being N and η_H the number of piles and the horizontal efficiency of the group, and $Q_1^{(\mathrm{lim,S})}=A\times\mu\times Q_3$, where A and μ are the soil-raft contact surface and the corresponding friction coefficient, respectively. As per the vertical load mechanism, it is assumed that pile's disconnection implies a null limit load upwards, whereas it does not alter the compressive bearing capacity. Note that in this simplified procedure the frictional interface influences the horizontal capacity of the group, but the soil located below the raft does not influence the vertical bearing capacity.

3.2 Ultimate capacity surface

The extended numerical framework was used to compute the failure loads for both conventional and frictionally disconnected foundation layouts. The corresponding ultimate capacity surfaces are represented in Figure

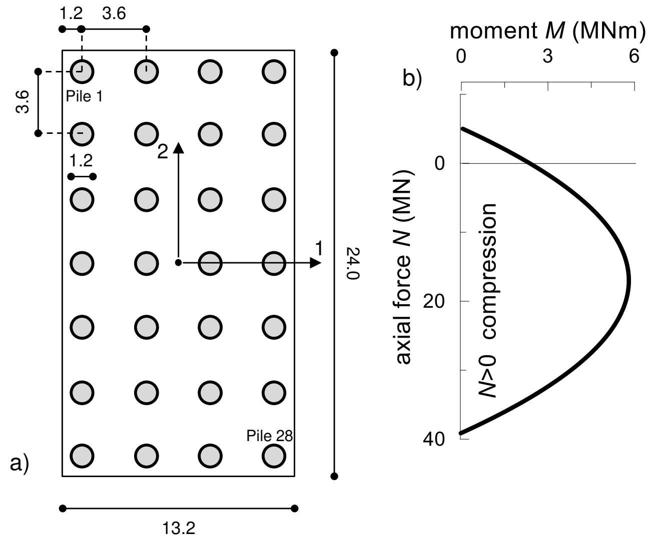

Figure 2. a) plan view of the foundation of pier P2 and b) relative N-M strength envelope of the pile cross section.

3 with reference, for brevity, to the sole space of the horizontal and vertical forces, Q_1 and Q_3 respectively, applied to the top of the foundation. Note that different scales are used for the Q_1 and Q_3 axes.

The frictionally disconnected foundation is characterised by a much smaller admissible domain because of three main effects: i) the lower horizontal resistance of the free-head piles compared to the fixed-head layout, ii) the attainment of the shearing resistance along the soil-raft contact and iii) the null limit value of the upwards load. For the foundation with connected piles, a horizontal load mechanism occurs for ratios $Q_1/Q_3>0.1$, whilst the vertical capacity of the group is the weak mechanism otherwise (Gorini and Callisto, 2022b). This result is partly confirmed for the case of disconnected piles, with the following distinction: a horizontal load mechanism occurs for $0.1<Q_1/Q_3<0.3$, while for relatively greater horizontal loads $Q_1/Q_3>0.3$ the ultimate conditions are controlled by the frictional resistance at the soil-raft interface.

The results of the simplified numerical framework were compared with the failure loads obtained through a coupled modelling of the soil-piles-raft system at hand (dotted lines) using OPTUM G3 (OptumCE, 2016). It is based on the application of the theorems of plastic limit analysis in finite element simulations (Sloan, 2013). In this analysis type both the soil domain and the piles were modelled using solid elements with a rigid-perfectly plastic behaviour described by the Mohr–Coulomb failure criterion, calibrated on the strength properties described in Section 2, with an associated flow rule. The numerical simulations computed the magnitude of the resultant load applied to the raft deriving from optimised lower and upper bound solutions. Several load paths were investigated: upward loading and four loading paths in which the horizontal load is increased at a constant level of the vertical force $Q_3/Q_3^{(+)}$ = 0, 0.05, 0.2, 0.4, where $Q_3^{(+)}$ is the compressive bearing capacity of the soil-piles system evaluated with DeepFUL (vertical stress transfer at the soil-raft contact neglected). The results at higher Q_3 levels are omitted, since the assumption of associativity of the plastic flow leads to a substantial overestimation of the limit load due to the excessive spreading of the bearing capacity-type mechanism at the pile tips. Each analysis is composed of several iterations with mesh adaptivity, so that the calculation stops when upper and lower bound solutions become close to each other and do not vary significantly.

The resulting limit loads are shown in Figure 3 (dotted lines), with reference to the sole upper bound solution computed in OPTUM. They are in agreement with the ovoidal shape of the ultimate locus provided by DeepFUL but yield larger values of the limit loads, as an effect of the conservatism introduced in the simplified solution. In particular, from the comparison between the Optum and DeepFUL results it can be inferred

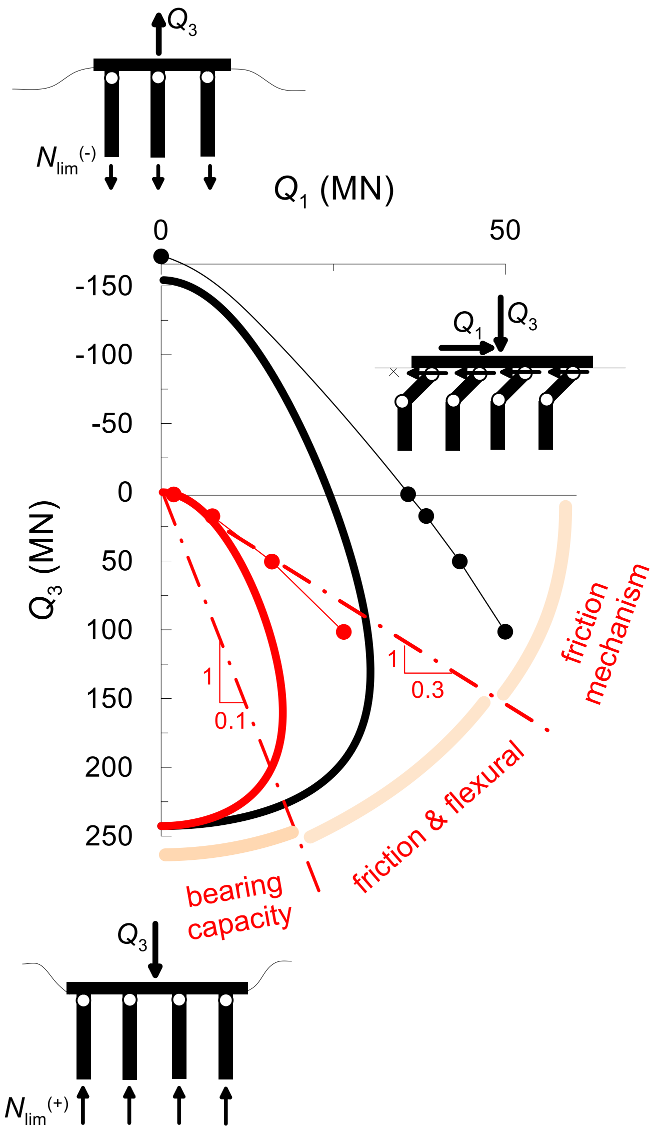

Figure 3. Force combinations Q_1-Q_3 causing failure of the basic (in black) and dissipative (in red) layouts of the reference piled foundation, obtained with DeepFUL (continuous lines) and through coupled finite-element limit analysis (dotted lines).

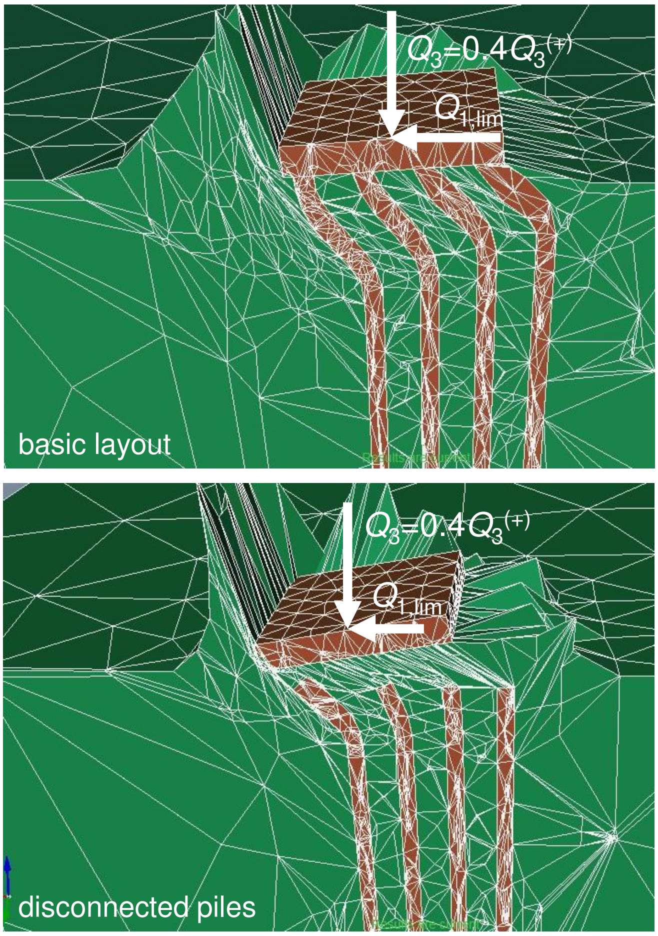

Figure 4. Central section view of the deformed mesh associated with the kinematic failure mechanisms of the reference pile group and the dissipative layout (interface friction angle = 25°), obtained through finite element limit analysis in the case of a combined load Q_1-Q_3, with $Q_3=0.4\times Q_3^{(+)}$.

that the contribution to the vertical downward capacity of the soil in contact with the raft is the main cause of discrepancy. In fact, the differences between the two modelling techniques become minimal when the vertical load is directed upwards (no contribution of the raft) while magnify for downward loads (the raft transfers contact stresses to the soil).

Figure 4 compares the OPTUM G3 plastic mechanisms associated with the upper bound solution for $Q_3/Q_3^{(+)} = 0.4$, with or without the piles disconnection. In both cases, a limited portion of the foundation soil is involved in the mechanism. The deformation pattern of the foundation system at failure changes radically as an effect of the piles disconnection: it combines the sliding of the raft and the attainment of the flexural capacity in some piles according to a free-head long-pile mechanism, with a depth of the plastic hinge marginally depending on the position of the pile. In a more general way, the totality of the Optum results, omitted for brevity, showed that the horizontal load mechanisms can be grouped into three typologies:

- *friction-based mechanism*, associated with the sole relative sliding of the raft on the soil, occurring for $Q_3/Q_3^{(+)}<0.3$;
- *partial friction-flexural mechanism*, implying the relative sliding along the dissipative interface and the attainment of the flexural capacity only in some piles, for $0.3<Q_3/Q_3^{(+)}<0.8$;
- *mixed friction-flexural mechanism*, relative to the combined attainment of the resistance at the soil-raft contact and in all piles, for $Q_3/Q_3^{(+)}>0.8$.

The considerations above, obtained through a refined modelling of the entire system, provide a view to the failure modes occurring for the considered frictionally disconnected piled foundation, and confirm the assumptions introduced in the simplified numerical framework (see Section 3.1).

4 A MACROELEMENT FOR FRICTIONALLY DISCONNECTED PILED FOUNDATIONS

The results obtained in the previus sections were used to develop a macroelement representation for friction piled foundations, called F-SPME (Friction Soil-Piles Macroelement), intended as a relationship between the generalised forces, Q_i (three forces and two moments, neglecting the moment around the vertical axis), exchanged between the foundation raft and the superstructure, and the corresponding displacements and rotations, q_i. The elastic-plastic response of the model is derived within a novel analysis method, called TIM approach (Gorini and Callisto, 2022a; Gorini and Callisto, 2023; Gorini et al., 2023). In this method, Thermodynamic Inertial Macroelements (TIMs) simulate, at a residual computational demand, the response of geotechnical systems in the assessment of structures, accounting for nonlinear and frequency-dependent features under multiaxial loading. A TIM is formulated as a multi-surface constitutive law with kinematic hardening developed using a rigorous thermodynamic framework, commonly called hyperplasticity (Collins and Houlsby, 1997).

The incremental response of the F-SPME is fully defined by two consistent potentials: it has the same energy function as the other TIMs, but a different dissipation function. The latter is a function of the yield surfaces of the model under the assumptions of associativity of the plastic flow and validity of the orthogonality principle (Ziegler, 1977). The yield surfaces are assumed homotetic with each other and present an increasing size from the innermost one, of first yield, to the ultimate capacity surface described by a five-dimensional generalisation of the locus obtained in Section 3.2.

The calibration of the F-SPME requires three fundamental ingredients: the ultimate capacity, delimiting the plastic domain, the initial stiffness and the participating masses of the soil-foundation system under multiaxial loading, characterising the small-strain frequency-dependant response. The participating mass along the i^{th} global degree of freedom of the foundation can be obtained from the respective values of the small-strain stiffness and vibration period, following an analogous procedure to the one delineated for foundations with connected piles (Gorini and Callisto, 2023). In detail, the small-strain participating masses are taken equal to the ones of the layout with connected piles along the vertical and rotational degrees of freedom of the foundation, whereas in the horizontal direction it is assumed equal to the mass of the raft as in this case soil inertia is negligible compared to the one of the raft.

The F-SPME was implemented in the finite element analysis framework OpenSees (McKenna et al., 2000) as a new member of the *NDTIMaterial*-class collecting the TIMs (Gorini et al., 2023). The new C++ source code includes the multiaxial constitutive relationship of the model. In the numerical model of a structural system with TIMs, the material is assigned to the zero-length finite element *ZeroLength6D* (Gorini and Callisto, 2023) establishing an explicit, translational-rotational relationship between two overlapped nodes.

In the structural analysis, during the static stages, for instance representing the construction sequence, the end node of the macroelement is fully restrained. Under seismic loading, the F-SPME is combined with the participating masses of the foundation, the latter assigned to the base node of the generic column in the global structural model. The end node of the F-SPME is subjected to a multi-component input motion, evaluated through a free-field ground response analysis at an effective depth of $10D$, where D is the pile diameter.

5 REPERCUSSIONS ON STRUCTURAL PERFORMANCE

The seismic performance of the bridge under examination is investigated using the extended TIM approach, that is by carrying out dynamic analyses in the time domain on the global structural model equipped with TIMs simulating soil-structure interaction. Two configurations of the geotechnical systems are compared: the conventional layouts and the ones with dissipative interface between raft and piles. The TIMs are subjected to a three-component seismic motion representing a Near-Collapse earthquake scenario for the case at hand (Gorini and Callisto, 2022a). The model was implemented in OpenSees, reproducing the highly nonlinear features of piers, bearing devices and soil-structure interaction. The use of the TIMs reduces the computational effort to a minimum, so that the analyses were carried out on a common laptop machine requiring a computation time of about 5 mins each.

The bridge performance is concisely illustrated in Figure 5 as the shear force-drift relationships of the bearing devices and the force-deformation responses of the geotechnical systems in the longitudinal direction, that were found to be the most vulnerable components under seismic loading. Compared to the standard layout (black trends), the enhanced dissipative response of the friction-based dissipative geotechnical systems (in red) magnifies irreversible deformations at the base of the superstructure. The abutments show a pronounced nonlinear response, enhanced by the attainment of the resistance along the dissipative interface. This is more evident for abutment A1 not connected with the deck

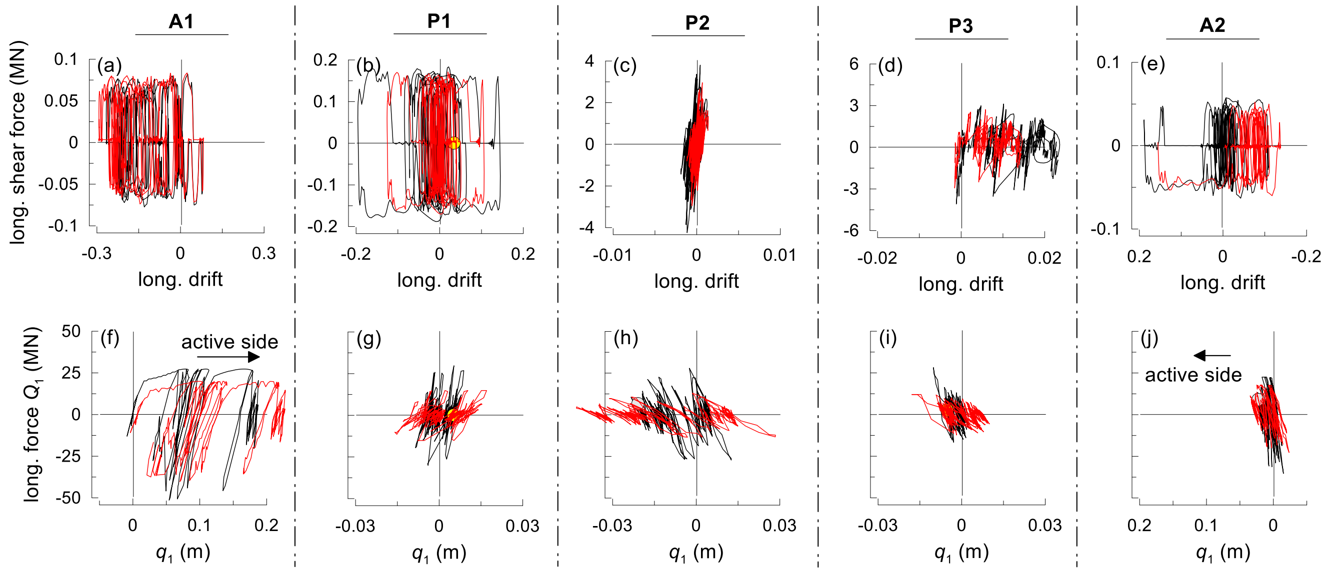

Figure 5. Comparison between the seismic performance of the reference bridge with and without friction dissipative foundations (red and black trends, respectively): a-e) shear force-drift relationship of the bearing devices and f-j) force-deformation responses of the geotechnical systems in the longitudinal direction.

longitudinally, in which the inertial forces coming from the embankment push permanently the abutment towards the centre of the bridge, with a minor increment of the displacement demand for the respective bearing.

The reduced ultimate capacity of the piers foundations with disconnected piles increases permanent displacements as well. In this case, however, the pronounced dissipative response of the foundations leads to a marked reduction in the displacement and ductility demands for the relative bearings supporting the deck.

6 CONCLUSIONS

The adoption of seismic-protection solutions at the level of the geotechnical systems is receiving an increasing attention, as it can efficiently mitigate the seismic actions transferred to the superstructure. In this regard, friction dissipative foundations can be easily implemented in soil-structure layouts, but their favourable performance requires careful design and assessment.

The introduction of a dissipative layer between piles and raft alters the failure modes of the foundation under multiaxial loading. Three types of global plastic mechanisms were detected, associated with a different involvement of the flexural capacity of the piles and of the sliding of the raft, that were seen to be related to the vertical load level.

The behaviour of frictionally disconnected piled foundations was integrated within a thermodynamic-based numerical approach (TIM), simulating nonlinear and frequency-dependant features of soil-structure interaction in the structural analysis through the macroscopic description of the soil-interface-foundation response.

The extended TIM approach was efficiently applied for assessing the performance of a typical tall viaduct having frictionally disconnected foundations. The dissipative interface at the piers foundations were seen to produce a favourable effect on the structural performance by virtue of the limitation in the shear forces transmitted to the superstructure. For the bridge abutments, instead, the effectiveness of the frictional disconnection was found to be only marginal. This is probably due to the substantial inertial forces developing in the approach embankment, that cannot be controlled by the frictional disconnection at the pile-raft interface. For the latter case, more appropriate solutions are currently under development to reach an optimised performance of bridges.

7 REFERENCES

Callisto, L., Gorini, D.N. 2020. Seismic behaviour of a suspension bridge with dissipative foundations, *Italian Geotechnical Journal*, **1/2020(1)**, 22-37, doi.org/10.19199/2020.1.0557-1405.022

Collins, I.F., Houlsby, G.T. 1997. Application of thermomechanical principles to the modelling of geotechnical materials, *Proc. Ro. Soc. – Math., Physical and Engineering Sciences*, The Royal Society, London, A, **453**, 1975-2001

Gorini, D.N., Callisto, L. 2019. Seismic performance and design approach for friction dissipative foundations, *Soil Dynamics and Earthquake Engineering*, **123**, 513-519

Gorini, D.N., Whittle., A.J., Callisto, L. 2019. Ultimate design capacity of bridge abutments, *Earthquake Geotechnical Engineering for Protection and Development of Environment and Constructions: Proceedings of the 7th International Conference on Earthquake Geotechnical Engineering, (ICEGE 2019)*, 2682-2689, Rome, Italy, DOI: 10.1201/9780429031274

Gorini, D.N., Callisto, L. 2022a. A class of thermodynamic inertial macroelements for soil-structure interaction, *In Springer Series in Geotechnical, Geological and Earthquake Engineering, proceedings of the 4th International Conference on: Performance based Design in Earthquake Geotechnical Engineering, Beijing*, China, 1095-1102, doi: 10.1007/978-3-031-11898-2_87

Gorini, D.N., Callisto, L. 2022b. Generalised ultimate loads for pile groups, *Acta Geotechnica* **17**, 2495-2516

Gorini, D.N., Callisto, L. 2023. A multiaxial inertial macroelement for deep foundations, *Computers and Geotechnics*, **155**.

Gorini, D.N., Callisto, L., Whittle, A.J. 2023. A multiaxial inertial macroelement for bridge abutments, *International Journal for Numerical and Analytical Methods in Geomechanics*, **47**, 793-816

Italian Building Code. 2018. *Norme Tecniche per le Costruzioni*. D.M. 17.01.2018. Italian Ministry of Infrastructures and Transportation, Rome.

Kim, D.S., Ko, K.W., Manandhar, S., Park, H.J., Ha, J.G. 2019. Dynamic centrifuge tests for soil-foundation-structure interaction problems: Disconnected Piled Raft (DPR), *Earthquake Geotechnical Engineering for Protection and Development of Environment and Constructions: Proceedings of the 7th International Conference on Earthquake Geotechnical Engineering, (ICEGE 2019)*, 105-120

Ko, K.W., Park, H.J., Ha, J.G., Jin, S., Song, Y.H., Song, M.J., Kim, D.S. 2018. Evaluation of dynamic bending moment of disconnected piled raft via centrifuge tests, *Canadian Geotechnical Journal* **56(12)**, 1917-1928

McKenna, F., Fenves, G.L., Scott, M.H., 2000. *Open system for earthquake engineering simulation*, http://opensees.berkeley.edu

OptumCE 2016. *OptumG2 v. 2016*. Manual, https://optumce.com/products/brochure-and-datasheet/

Pecker, A. 2003. Aseismic foundation design process, lessons learned from two major projects: the Vasco de Gama and the Rion Antirion bridges, *In the Proc. of ACI Int. Conf. Seismic Bridge Design & Retrofit*, La Jolla, California

Sloan, S.W. 2013. Geotechnical stability analysis. *Geotechnique*, **63(7)**, 531-572

Zhang, Y., Yao, S., Christie, S.R. 2013. Non-linear and equivalent linear site response analysis for the Izmit Bay bridge, *In the Proceedings of 3rd International FLAC /DEM Symposium*, paper 05/2, http://www.itascacg.com/sites/itascacg.com/files/documents/05-02.pdf

Ziegler, H. 1977. *An introduction to thermomechanics*, North Holland, Amsterdam